

Nucleon spin structure III: Origins of the generalized Gerasimov-Drell-Hearn sum rule

Wei Zhu and Jianhong Ruan

Department of Physics, East China Normal University, Shanghai 200062, P.R. China

Abstract

The generalized Gerasimov-Drell-Hearn (GDH) sum rule is understood based on the polarized parton distributions of the proton with the higher twist contributions. A simple parameterized formula is proposed to clearly present the contributions of different components in proton to $\Gamma_1^p(Q^2)$. We find that the contribution of quark helicity to $\Gamma_1^p(Q^2)$ is almost constant (~ 0.123); the twist-4 effect dominates the suppression of $\Gamma_1^p(Q^2)$ at $Q^2 < 3\text{GeV}^2$, while the twist-6 effect arises a dramatic change of $\Gamma_1^p(Q^2)$ at $Q^2 < 0.3\text{GeV}^2$, it implies a possible extended objects with size $0.2 - 0.3\text{ fm}$ inside the proton.

PACS number(s): 12.38.Cy, 12.38.Qk, 12.38.Lg

keywords: Nucleon spin structure

1 Introduction

The structure of nucleon is an important open question. The perturbative QCD (pQCD) at high energy has been proved a successful approach to describe the phenomena in terms of elementary quark and gluon constituents. On the other hand, hadronic processes at low transfer momentum are usually described by using meson and baryon degrees of freedom. Unfortunately, the transition from quark-gluon to hadron degrees of freedom remains shrouded in mystery.

There is particular interest in the first moment $\Gamma_1(Q^2) = \int_0^1 dx g_1(x, Q^2)$ of the spin structure functions $g_1(x, Q^2)$, which has been measured from high Q^2 down to $\sim 0 \text{ GeV}^2$. The goal of obtaining universal expressions describing $\Gamma_1(Q^2)$ at any Q^2 is an attractive task for both theoretical and phenomenological point of view. In theory, $\Gamma_1(0)$ is constrained by the Gerasimov-Drell-Hearn (GDH) sum rule [1,2]

$$I_1(0) = \lim_{Q^2 \rightarrow 0} \frac{2M^2}{Q^2} \Gamma_1(Q^2) = -\frac{\kappa^2}{4} \sim -0.8, \quad (1.1)$$

where κ is the anomalous magnetic moment of the nucleon. On the other hand, the Bjorken sum rule [3] says

$$\lim_{Q^2 \rightarrow \infty} [\Gamma_1^p(Q^2) - \Gamma_1^n(Q^2)] = \frac{1}{6} \left| \frac{g_A}{g_V} \right|, \quad (1.2)$$

this ratio is known very accurately [4]: $g_A/g_V = -1.2695 \pm 0.0029$.

The connection of the two sum rules by means of the generalized GDH sum rule is (For an overview see, for example Ref. [5])

$$I_1(Q^2) = \frac{2M^2}{Q^2} \Gamma_1(Q^2), \quad (1.3)$$

which allows us to study the transition between the perturbative partonic structure and non-perturbative hadronic picture of nucleon in lepton-nucleon scattering processes. The data show that this sum rule at low $Q^2 < 1 \text{ GeV}^2$ changes dramatically and exceeds the variation bound at higher Q^2 , which has been parameterized (but not explanation) in [6]. The explanation of the generalized GDH sum rule is an active subject. For example, the

phenomenological constituent quark model [7], the vector meson dominate (VMD) model [8], the resonance contributions [9], the chiral perturbation theory (χ PT) [10] are used to understand the generalized GDH sum rule.

The purpose of this work is try to expose the partonic structure in the generalized GDH sum rule. According to the parton model, the polarized structure functions of nucleon at $Q^2 > \text{a few } GeV^2$ and the leading order (LO) approximation are defined by the parton distributions as

$$g_1^{DGLAP}(x, Q^2) = \sum_i e_i^2 [\delta q_i(x, Q^2) + \delta \bar{q}_i(x, Q^2)], \quad (1.4)$$

where the polarized parton distributions obeys the DGLAP evolution equation [11]. In our previous works [12,13], the DGLAP equation with the parton recombination corrections [14,15] are used to derive the unpolarized and polarized parton distributions starting from simple initial valence quark distributions at $Q^2 \sim 0.064 GeV^2$. Our numerical calculations show that the predicted parton distributions consist with the data well both for polarized and unpolarized data at $Q^2 > 1 GeV^2$. Considering the nonperturbative corrections to the spin structure function at low Q^2 becoming important, Eq. (1.4) in the full Q^2 range should be generalized to

$$g_1^p(x, Q^2) = g_1^{DGLAP+ZRS}(x, Q^2) + g_1^{VMD}(x, Q^2) + g_1^{HT}(x, Q^2), \quad (1.5)$$

where $g_1^{DGLAP+ZRS}(x, Q^2)$ is the solutions of the DGLAP equation with the parton recombination (ZRS) corrections at the $LL(Q^2)$ approximation [15], while $g_1^{VMD}(x, Q^2)$ is the contributions of the vector meson in virtual photon via the vector meson dominated (VMD) model [16], and $g_1^{HT}(x, Q^2)$ is the higher twist corrections. The corresponding first moment of g_1^p is

$$\Gamma_1^p(Q^2) = \Gamma_1^{DGLAP+ZRS}(Q^2) + \Gamma_1^{VMD}(Q^2) + \Gamma_1^{HT}(Q^2). \quad (1.6)$$

Since we have known the contributions of $g_1^{DGLAP+ZRS}$ and g_1^{VMD} , one can expose the properties of $\Gamma_1^{HT}(Q^2)$ after subtracting these two contributions from the experimental

data about $\Gamma_1^p(Q^2)$. This opens a window to visit higher twist effects at low Q^2 in the nucleon structure. We find that (i) the contributions of quark helicity to $\Gamma_1^p(Q^2)$ are almost constant (~ 0.123); (ii) the negative twist-4 effect dominates the suppression of $\Gamma_1^p(Q^2)$ at $Q^2 < 3\text{GeV}^2$, while the twist-6 effect becomes positive at $Q^2 \sim 1\text{GeV}^2$ and it arises a dramatic change of $\Gamma_1^p(Q^2)$ at $Q^2 < 0.3\text{GeV}^2$, these effects can be described by a simple parameterized form; (iii) the slope of the higher twist coefficient suddenly enhance at $Q^2 \sim 1\text{GeV}^2$, which is near an estimation of the constituent quark scale $0.2 \sim 0.3\text{fm}$.

We will give a review of the structure functions in full Q^2 range based on the partonic picture in Sec. 2, where the contributions of parton helicity and the VMD mechanism in our previous works are summarized. Then we extract the twist-4 and 6 corrections to $\Gamma_1^p(Q^2)$ in Sec. 3, which expose the interesting change of the partonic structure of proton at the low Q -scales. The discussions and a summary are presented in Sec. 4.

2 Spin structure functions in the full Q^2 range

We have detailed the first two terms of Eq. (1.5) in our previous two works [13,16]. $g_1^{DGLAP+ZRS}$ are the contributions of parton helicities obeying the DGLAP equation with the parton recombination corrections [14,15], where the input valence quark distributions at $\mu^2 = 0.064 GeV^2$ have been fixed through a global fitting:

$$xu_v(x, \mu^2) = 24.30x^{1.98}(1-x)^{2.06}, \quad (2.1)$$

$$xd_v(x, \mu^2) = 9.10x^{1.31}(1-x)^{3.80}, \quad (2.2)$$

for unpolarized parton distributions, and

$$\delta u_v(x, \mu^2) = 40.3x^{2.85}(1-x)^{2.15}, \quad (2.3)$$

$$\delta d_v(x, \mu^2) = -18.22x^{1.41}(1-x)^{4.0}, \quad (2.4)$$

for polarized parton distribution. The input distributions Eqs.(2.1-2.4) neglect the contributions of asymmetry sea quark contributions in this work. We consider these corrections to Γ_1 are small.

Using Eqs. (2.1-2.4) we obtain $\Gamma^{DGLAP+ZRS}(Q^2) \simeq 0.123$, which seems insensitive to the complicated behavior of g_1^p at small x [16].

Note that $1/\mu = 0.78 fm$ consists with a typical proton scale $0.8 \sim 1 fm$. We assume that μ is a minimum average transverse momentum of the partons in the proton due to the uncertainty principle. Thus, we assume that the Q^2 -dependence of parton distributions are freezed at $Q^2 < \mu^2$. Using this assumption we avoid the un-physical singularities at $Q \sim \Lambda_{QCD}$. The dashed curve in Fig. 1 is our predicted $\Gamma_1^{DGLAP+ZRS}(Q^2)$. We find that it is almost irrelevant to Q^2 .

The second term of Eq. (1.5) is the the contributions from the interaction of ρ - and ω -mesons in the virtual photon with the proton and they are described by the vector meson dominance (VMD) model [17],

$$xg_1^{VMD}(x, Q^2) = \frac{Q^2}{8\pi} \sum_v \frac{m_v^4 \Delta\sigma_{vp}(s)}{\gamma_v^2 (Q^2 + m_v^2)^2}. \quad (2.5)$$

In this formula the constants γ_v are determined by the leptonic widths of the vector mesons and m_v denotes the mass of ρ and ω at $Q^2 < 1\text{GeV}^2$. The cross-sections $\Delta\sigma_v(s)$ are the unknown cross sections for the scattering of polarized mesons and nucleons. s is the CMS energy squared for the γp collision and $s \sim Q^2/x$. In work [16] we assume

$$g_1^{VMD}(x, Q^2) = B \frac{(m_V^2)^{2-\lambda+\epsilon} Q^{2\lambda}}{(Q^2 + m_V^2)^2} \left[\left(\frac{x}{x_0}\right)^{-\lambda+\epsilon} \theta(x_0 - x) + \frac{\ln^4 x}{\ln^4 x_0} \theta(x - x_0) \right], \quad (2.6)$$

$\lambda = 1$ and ϵ is a small positive parameter due to the requirement of integrability of g_1^p at $x \rightarrow 0$. Thus, we have

$$\Gamma_1^{VMD}(Q^2) = \int_0^1 dx g_1^{VMD}(x, Q^2) \simeq A \frac{m_v^2 Q^2}{(Q^2 + m_v^2)^2}, \quad (2.7)$$

where we take $A = 0.162$, which corresponds to $\epsilon = 0.018$. The solid curve in Fig. 1 is $\Gamma_1^{DGLAP+ZRS}(Q^2) + \Gamma_1^{VMD}(Q^2)$, it shows a weaker Q^2 -dependence at $Q^2 > 1\text{GeV}^2$.

Comparing the solid curve with $\Gamma_1^p(Q^2)$ data [20-22] in Fig. 1, one can expect that the higher twist corrections g_1^{HT} play a significant role at low Q^2 to the general GDH sum rule. We will detail them in next section.

3 Higher twist contributions to the GDH sum rule

According to the operator product expansion (OPE), the appearance of scaling violations at low Q^2 is related to the higher twist corrections to moments of structure functions. Higher twists are expressed as matrix elements of operators involving nonperturbative interactions between quarks and gluons. The study of higher twist corrections gives us a direct insight into the nature of long-range quark-gluon correlations. The higher twist corrections to g_1 have several representations. The initial parton recombination corrections have been examined in our works [12,13]. The VMD model was used to simulate a special higher twist effect in our previous work [16]. In this work, we will try to expose the remaining power suppression corrections to Γ_1^p . For this sake, we make $\Gamma_1^p(Q^2)$ (i.e., the data points [28-20] in Fig. 1)- $[\Gamma_1^{DGLAP+ZRS}(Q^2) + \Gamma_1^{VMD}(Q^2)]$ (i.e., the solid curve in Fig. 1). Figure 2 shows such a result at $Q^2 > 0.2 \text{ GeV}^2$, which has been smoothed with minimum $\chi^2/D.o.f.$.

To expose the possible physical information of the curve in Fig. 2, according to QCD operator product $1/Q^2$ -expansion,

$$\Gamma_1^{HT}(Q^2) = \sum_{i=2}^{\infty} \frac{\mu_{2i}(Q^2)}{Q^{2i-2}}, \quad (3.1)$$

we take first three approximations

$$\Gamma_1^{HT(4)}(Q^2) = \frac{\mu_4(Q^2)}{Q^2}, \quad (3.2)$$

$$\Gamma_1^{HT(4+6)}(Q^2) = \frac{\mu_6(Q^2) + \mu_4(Q^2)Q^2}{Q^4}, \quad (3.3)$$

$$\Gamma_1^{HT(4+6+8)}(Q^2) = \frac{\mu_8(Q^2) + \mu_6(Q^2)Q^2 + \mu_4(Q^2)Q^4}{Q^6}. \quad (3.4)$$

Then we plot the curves $Q^2\Gamma_1^{HT(4)}(Q^2)$, $Q^4\Gamma_1^{HT(4+6)}(Q^2)$ and $Q^6\Gamma_1^{HT(4+6+8)}(Q^2)$ in Fig.

3. There are following interesting properties of these results:

(i) $Q^6\Gamma_1^{HT(4+6+8)}(Q^2) \rightarrow 0$, if $Q^2 \rightarrow 0$. This implies that μ_8 vanishes if it is independent of Q^2 . Therefore, $\Gamma_1^{HT(4+6)}(Q^2)$ is an appropriate approximation.

(ii) Three curves in Fig. 3 cross at a same point $Q^2 \sim 1\text{GeV}^2$. Particularly, the intercept μ_6 of the line, which cuts $Q^4\Gamma_1^{HT(4+6)}(Q^2)$ suddenly changes its sing from -0.03 at $Q^2 > 1\text{GeV}^2$ to 0.01 at $Q^2 < 1\text{GeV}^2$. This result exposes that the correlation among partons in the proton has an obvious change near $Q \sim 1\text{GeV}$.

(iii) Although $\Gamma_1^{HT}(Q^2) \sim \Gamma_1^{HT(4)}(Q^2) = -0.05/Q^2$ is an acceptable approximation at $Q^2 > 1.5\text{GeV}^2$, the correct choose is $\Gamma_1^{HT}(Q^2) = \Gamma_1^{HT(4+6)}(Q^2)$. We use

$$\Gamma_1^{HT(4+6)}(Q^2) = \frac{\mu_4}{Q^2 + \epsilon^2} + \frac{\mu_6}{Q^4 + \epsilon^4} \quad \text{at } Q^2 < 0.3\text{GeV}^2 \quad (3.5)$$

to fit the data at $Q^2 < 0.3\text{GeV}^2$, where we add a parameter ϵ to remove the unnatural singularity at $Q^2 = 0$. The value of ϵ is sensitive to $I(0)$. We find that $\mu_4 = -0.154$, $\mu_6 = 0.037$ and $\epsilon^2 = 0.32\text{GeV}^2$. On the other hand, the negative twist-4 effect dominates the suppression of $\Gamma_1^p(Q^2)$ at $Q^2 < 3\text{GeV}^2$, while the twist-6 effect change its sing at $Q^2 = 1\text{GeV}^2$ and its positive effect arises a dramatic change of $\Gamma_1^p(Q^2)$ at $Q^2 < 0.3\text{GeV}^2$.

In summary,

$$\Gamma_1^p(Q^2) = 0.123 + 0.162 \frac{m_v^2 Q^2}{(Q^2 + m_v^2)^2} + \Gamma_1^{HT}(Q^2) \quad (3.6)$$

where the HT contributions are

$$\Gamma_1^{HT}(Q^2) = \begin{cases} -\frac{0.043/M^2}{Q^2} - \frac{0.03/M^2}{Q^4} & \text{at } Q^2 > 1\text{GeV}^2 \\ -\frac{0.0844/M^2}{Q^2} + \frac{0.0114/M^2}{Q^4} & \text{at } 0.3 < Q^2 < 1\text{GeV}^2 \\ -\frac{0.156/M^2}{Q^2+0.32} + \frac{0.037/M^2}{(Q^2+0.32)^2} & \text{at } Q^2 < 0.3\text{GeV}^2 \end{cases} \quad (3.7)$$

where $M^2 = 1\text{GeV}^2$ is the Borel parameter used in the sum rule. We present the comparison of our $\Gamma_1^p(Q^2)$ with the data [18-20] in Fig. 4. The corresponding $I_1^p(Q^2)$ using Eqs. (1.3), (3.6) and (3.7) is presented in Fig. 5.

4 Discussions and summary

(i) The parton-hadron duality was first noted by Bloom and Gilman [21] in deep inelastic scattering (DIS) and has been confirmed by many measurements. At low energies (or intermediate Bjorken variable x and low Q^2) DIS reactions are characterized by excitation of nucleon resonances; while at high virtuality such processes have a partonic description. The smooth high-energy scaling curve essentially reproduces the average of the resonance peaks seen at low energies. Burkert and Ioffe [6] indicated that the contribution of the isobar $\Delta(1232)$ electroproduction at small Q^2 can describe the general GDH sum rule, and they gave

$$\frac{\mu_4}{M^2} = -0.056 \sim -0.063, \text{ at } Q^2 = 0.3 \sim 0.8 \text{ GeV}^2 \quad (4.1)$$

$$\frac{\mu_6}{M^2} = 0.010 \sim 0.011, \text{ at } Q^2 = 0.3 \sim 0.8 \text{ GeV}^2, \quad (4.2)$$

which are compatible with our prediction Eq. (3.7).

Our results in Fig.3 indicates the slope of the twist coefficient $\mu_4(Q^2)$ in Eq. (3.7) suddenly enhance at $Q^2 \sim 1 \text{ GeV}^2$. It implies that the correlation among partons become stronger at scale $\sim 0.2 \text{ fm}$. We noted that Petronzio1, Simula and Ricco [22] reported that the inelastic proton data obtained at Jefferson Lab exhibit a possible extended objects with size of $\simeq 0.2 - 0.3 \text{ fm}$ inside the proton.

As we have shown that the twist $N > 6$ corrections are neglected at low Q^2 . This supports our generalized leading order (GLO) approximation [13,16]: if the lower order contributions are compatible with the experimental data at low Q^2 , one can image that the higher order corrections are cancelable each other.

In summary, we assume that the parton distributions are still available at $Q^2 < 1 \text{ GeV}^2$. Using the DGLAP equation with the parton recombination corrections, we indicate that the contributions of Q^2 -dependent parton distributions to the lowest moment of the spin-dependent proton structure function are almost constant in full Q^2 range. In the meantime, the contributions of a VMD-type nonperturbative part are isolated. After

removing the above two contributions from the existing experimental data for $\Gamma_1^p(Q^2)$, the higher twist power corrections present their interesting characters: parton correlations at $Q^2 \sim 1 \text{ GeV}^2$ and $\sim 0.3 \text{ GeV}^2$ show two bend points, where the twist-4 effect dominates the suppression of $\Gamma_1^p(Q^2)$ at $Q^2 < 3\text{GeV}^2$, while the twist-6 effect arises a dramatic change of $\Gamma_1^p(Q^2)$ at $Q^2 < 0.3\text{GeV}^2$. Within the analytic of these results, we are able to achieve a rather good description of the data at all Q^2 values using a simple parameterized form of $\Gamma_1^p(Q^2)$.

References

- [1] S.B. Gerasimov, Sov. J. Nucl. Phys. **2**, 430 (1966).
- [2] S.D. Drell and A.C. Hearn, Phys. Rev. Lett. **16**, 908 (1966).
- [3] J.D. Bjorken, Phys. Rev. **148**, 1467 (1966).
- [4] Particle Data Group, S. Eidelman et al., Phys. Lett. **B592**, 1 (2004).
- [5] D. Drechsel, S.S. Kamalov and L. Tiator, Phys. Rev. **D63**, 114010 (2001) hep-ph/0008306.
- [6] M. Anselmino, B.L. Ioffe and E. Leader, 1989, Sov. J. Nucl. Phys. **49**, 136 (1989); V.D. Burkert and B.L. Ioffe, Phys. Lett. **B296**, 223 (1992); J. Soffer and O.V. Teryaev, Phys. Rev. Lett. **70**, 3373 (1993); J. Soffer and O. Teryaev, Phys. Rev. **D70**, 116004 (2004).
- [7] D. Drechsel and L. Tiator Ann. Rev. Nucl. Part. Sci. **54**, 69 (2004), nucl-th/0406059; M. Gorchtein, D. Drechsel, M.M. Giannini, E. Santopinto and L. Tiator, Phys. Rev. **C70**, 055202 (2004) 055202, hep-ph/0404053.
- [8] B. Badelek, J. Kiriyluk, and J. Kwiecinski Phys. Rev. **D61**, 014009, hep-ph/9907569; B. Badelek, J. Kwiecinski and B. Ziaja, Eur. Phys. J. **C26**, 45 (2002), hep-ph/0206188.
- [9] D. Burkert and Z.J. Li, Phys. Rev. **D47**, 46 (1993)..
- [10] V. Bernard, Prog. Part. Nucl. Phys. **60**, 82 (2006); V. Bernard et al., Phys. Rev. **D67**, 076008 (2003); X. Ji et al., Phys. Lett. **B472**, 1 (2000).
- [11] G. Altarelli and G. Parisi, Nucl. Phys. **B126**, 298 (1977); V.N.Gribov and L.N. Lipatov, Sov. J. Nucl. Phys. **15**, 438 (1972); Yu.L.Dokshitzer, Sov. Phys. JETP. **46**, 641 (1977).

- [12] X.R. Chen, J.H. Ruan, R. Wang, P.M. Zhang and W. Zhu, Int. J. Mod. Phys. **E23**, 1450057 (2014), hep-ph/1306.1872.
- [13] W. Zhu and J.H. Ruan, Nucleon spin structure I: a dynamical determination of polarized gluon distribution in the proton, this serious works.
- [14] W. Zhu, Nucl. Phys. **B551**, 245 (1999), hep-ph/9809391; W. Zhu, J.H. Ruan, Nucl. Phys. **B559**, 378 (1999), hep-ph/9907330v2.
- [15] W. Zhu, Z.Q. Shen and J.H. Ruan, Nucl.Phys. **B692**, 417 (2004), hep-ph/0406212v2.
- [16] W. Zhu and J.H. Ruan, Nucleon spin structure II: spin dependent structure function g_1^p at small x , this serious works.
- [17] J. Sakurai, Currents and Mesons (The University of Chicago Press, Chicago, 1969);
- [18] HERMES Collaboration, A. Airapetian et al., Eur. Phys. J. C26 (2003) 527, hep-ex/0210047; Phys. Rev., **D75**, 012007 (2007).
- [19] E143 Collaboration, K. Abe et al., Phys. Rev. Lett. **78**, 815 (1997), hep-ex/9701004.
- [20] CLAS Collaboration, R. Fatemi et al., Phys. Rev. Lett. **91**, 222002 (2003), nucl-ex/0306019; K. V. Dharmawardane et al., Phys. Lett. **B641**, 11 (2006); P. E. Bosted et al., Phys. Rev. **C75**, 035203 (2007); Y. Prok et al., Phys. Lett. **B672**, 12 (2009).
- [21] E.D. Bloom and E.J. Gilman, Phys. Rev. Lett. **25**, 1140 (1970); Phys. Rev. **D4**, 2901 (1971).
- [22] M.Bacchi, L.Feretti, G.Giovannini, F.Govoni, Astron. Astrophys. **400**, 465 (2003), hep-ph/0301206.
- [23] M. Glück, E. Reya, and A. Vogt, Eur. Phys. J. **C5**, 461 (1998); M. Glück, E. Reya, M. Stratmann, W. Vogelsang, Phys.Rev. **D63**, 094005 (2001).

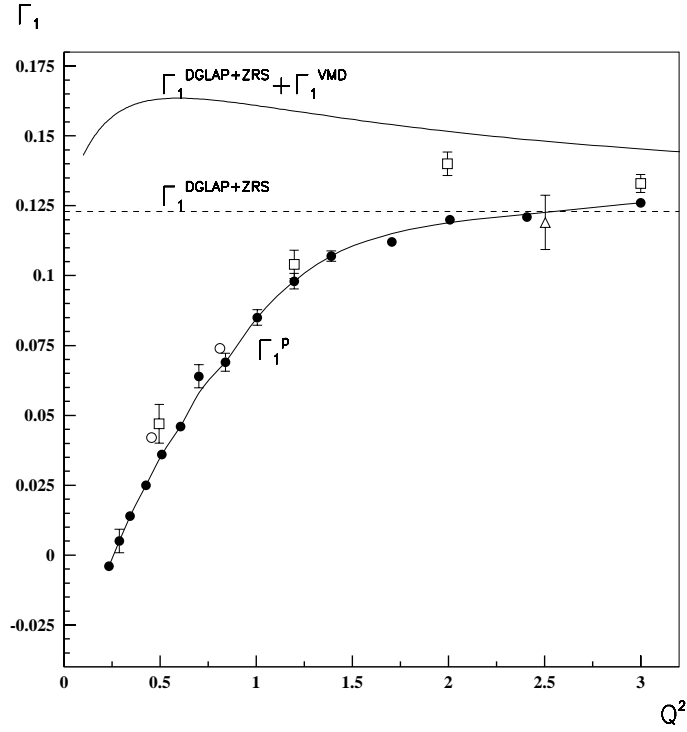


Figure 1: Contribution of quark helicity $\Gamma_1^{DGLAP+ZRS}(Q^2)$ (dashed curve) and combining VMD contribution $\Gamma_1^{DGLAP+ZRS}(Q^2) + \Gamma_1^{VMD}(Q^2)$ (solid curve). Data are from from Hermes experiment at DESY [18], the E143 experiment at SLAC [19] and the EG1a experiment using the CLAS detector at JLab [20].

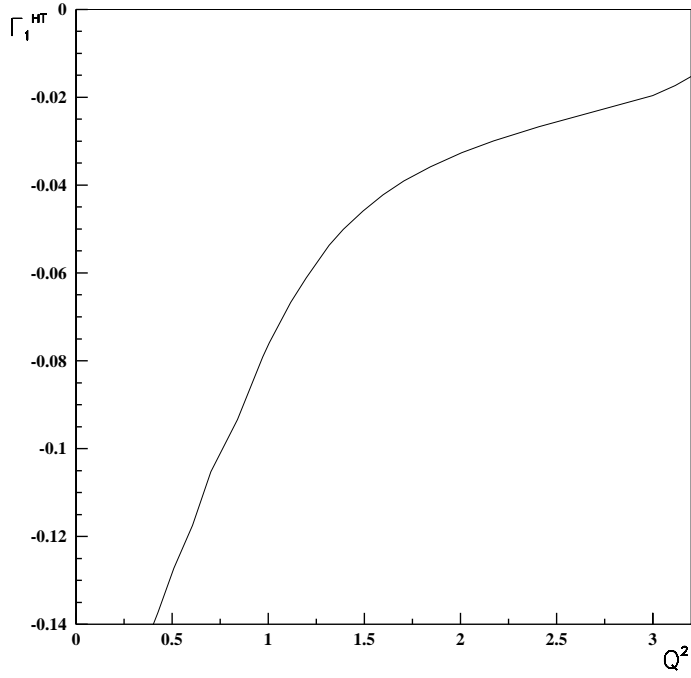


Figure 2: Contribution of higher twist $\Gamma_1^{HT}(Q^2)$ (smoothed curve) is taken from data-
 $[\Gamma_1^{DGLAP+ZRS}(Q^2) + \Gamma_1^{VMD}(Q^2)]$.

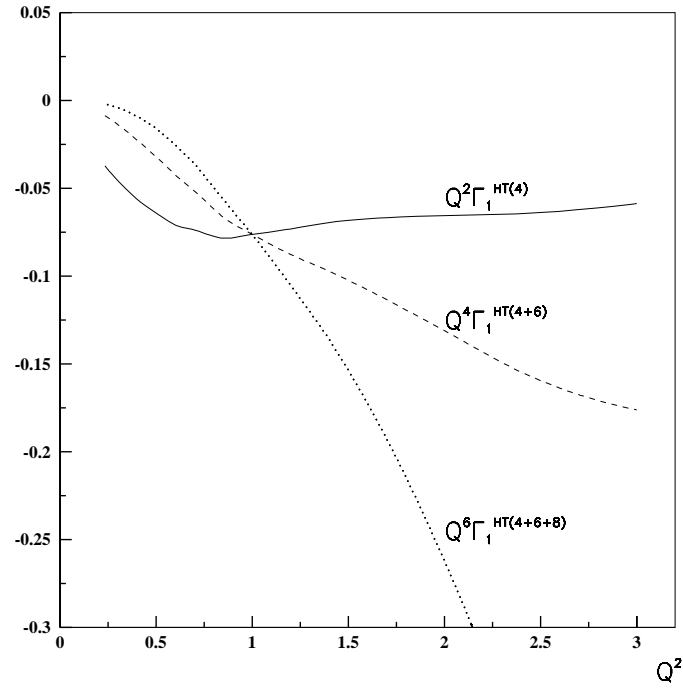


Figure 3: Three different analysis of the higher twist contributions.

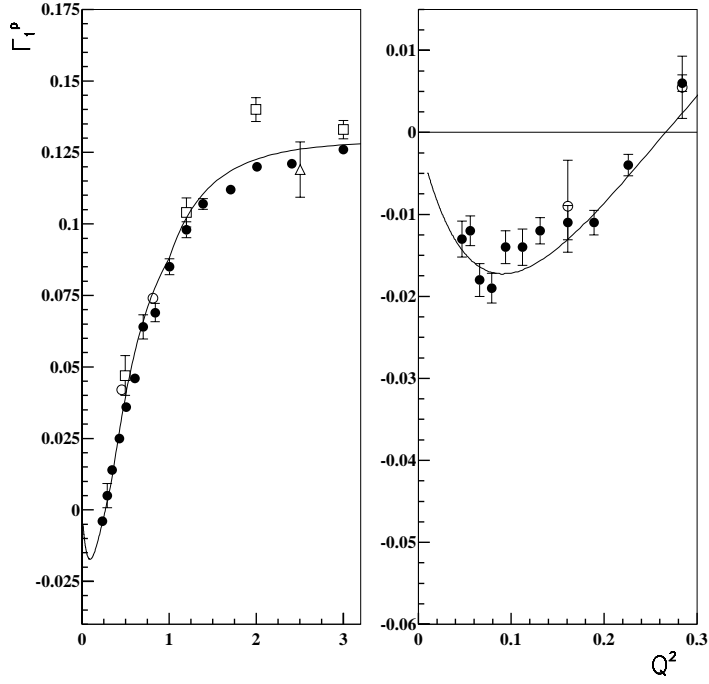


Figure 4: The Q^2 dependence of $\Gamma_1^p(Q^2)$ calculated by Eqs. (3.6) and (3.7). The data are taken from [18-20].

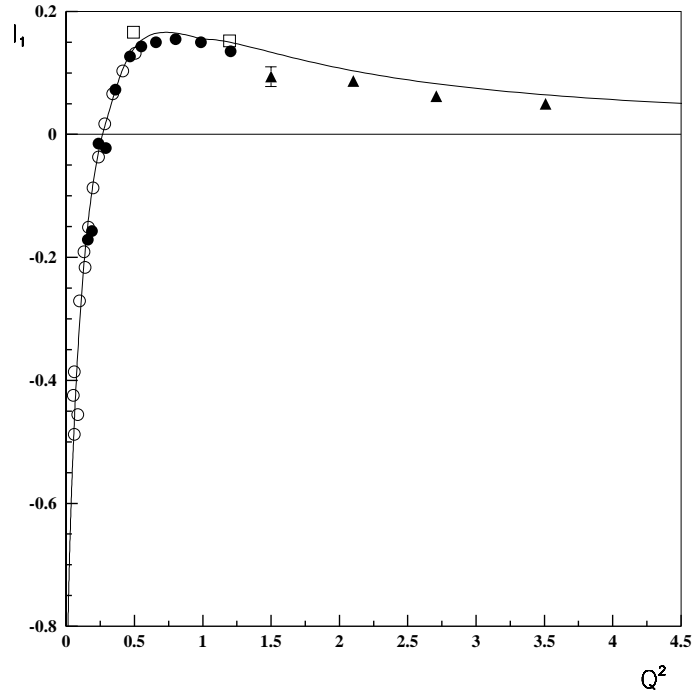


Figure 5: The Q^2 dependence of $I_1^p(Q^2)$ calculated by Eqs. (1.3), (3.6) and (3.7). The data are taken from [18-20].